2023-01-1431 Published 15 Jun 2023



Airborne Platform for Ice-Accretion and Coatings Tests with Ultrasonic Readings (PICTUR)

Leonid Nichman, Dan Fuleki, Naiheng Song, Ali Benmeddour, Mengistu Wolde, and David Orchard National Research Council Canada

Edgar Matida Carleton University

Kenny Bala, Zhigang Sun, Natalia Bliankinshtein, and Keyvan Ranjbar National Research Council Canada

Stephanie DiVito Federal Aviation Administration

Citation: Nichman, L., Fuleki, D., Song, N., Benmeddour, A. et al., "Airborne Platform for Ice-Accretion and Coatings Tests with Ultrasonic Readings (PICTUR)," SAE Technical Paper 2023-01-1431, 2023, doi:10.4271/2023-01-1431.

Received: 30 Nov 2022 Revised: 28 Apr 2023 Accepted: 30 Apr 2023

Abstract

azardous atmospheric icing conditions occur at sub-zero temperatures when droplets come into contact with aircraft and freeze, degrading aircraft performance and handling, introducing bias into some of the vital measurements needed for aircraft operation (e.g., air speed). Nonetheless, government regulations allow certified aircraft to fly in limited icing environments. The capability of aircraft sensors to identify all hazardous icing environments is limited. To address the current challenges in aircraft icing detection and protection, we present herein a platform designed for in-flight testing of ice protection solutions and icing detection technologies. The recently developed Platform for Ice-accretion and Coatings Tests with Ultrasonic Readings (PICTUR) was evaluated using CFD simulations and installed on the National Research Council Canada (NRC) Convair-580 aircraft that has flown in icing conditions over North East

USA, during February 2022. This aircraft is a flying laboratory, equipped with more than 40 sensors providing a comprehensive characterization of the flight environment including measurements of temperature, pressure, wind speed and direction, water droplet size and number distribution, and hydrometeor habits imagery. The flight tests of the platform included assessment of passive icephobic coatings as well as heat-assisted tests. Monitoring tools included visual high resolution, real-time inspection of the surface as well as detection of surface ice using NRC's Ultrasonic Ice Accretion Sensors (UIAS). In this paper, we present the new platform and show some preliminary commissioning results of PICTUR, collected inflight under, predominantly, supercooled small droplets and supercooled large drops (SLD) icing conditions. The combination of the platform and the complementary sensors on the aircraft demonstrated an effective and unique technique for icing studies in a natural environment.

Introduction

ircraft icing by supercooled water droplets pose a major hazard for aviation [1]. Up until 2015, the maximum icing envelopes used for the certification of transport category airplanes have been performed in accordance with the Title 14 Code of Federal Regulations (CFR) Part 25 Appendix C [2] that defines the icing environments with a median volume diameter (MVD) up to 40 μm for continuous maximum (stratiform clouds) and up to 50 μm for intermittent maximum (cumuliform clouds). However, following the accident of an ATR-72 at Roselawn, Indiana in 1994, the National Transport Safety Board report [3] concluded that the 14 CFR Part 25 Appendix C icing envelope has limitations regarding certification in conditions that contain supercooled large drops (SLD) with MVDs in excess of 100 μm .

In order to better understand the SLD environment, a series of international collaborative projects were conducted to measure and assess aircraft icing conditions that contain SLD [4–8]. The data provided by these studies have led to a greater understanding of the icing environment and enabled the expansion of the icing certification requirements to encompass SLD conditions through addition of Appendix O to 14 CFR Part 25 [9, 10]. In parallel with the development of new regulations related to flight in SLD icing, work was also conducted by several working groups to investigate mixed phase and fully glaciated conditions that posed significant threat to engine operation, with rollback, flameout, stall and core damage symptomatic of some events [11]. This work resulted in a further addition to the aircraft icing regulations with Appendix D to FAA's 14 CFR Part 33 [9, 12] and Appendix

P to EASA's Certification Specifications and Acceptable Means of Compliance for Large Aeroplanes (CS-25) [13].

Mitigation strategies against aircraft icing include navigating the aircraft away from the hazardous regions or grounding the aircraft, however this is not always possible due to the indiscernibility of the hazardous freezing layers by the commonly used aircraft instrumentation, ground and space remote-sensing and the operational and financial limitations (e.g., remaining fuel, flight cancellation and rerouting implications).

In practice, when aircraft fly through clouds at ambient temperatures below freezing, supercooled water droplets suspended in the cloud can impact and cause ice accretion, for example, on the fuselage and instrumentation, resulting in false and misleading flight data. Ice can also accrete on aircraft lift and control surfaces, most crucially on the leading edge of a wing, on the tail and around the engine intakes. Ice build-up can have a significant impact on the aircraft aerodynamics, through loss of lift and increase in drag, and can lead to catastrophic failure of the aircraft [e.g., 14, 15]. One of the deadliest examples of icing hazard is the loss of Air France flight 447 (2009), taking 228 lives due to icing of aircraft pitot tube in high ice water content (HIWC) conditions. Even more recently, there have been numerous other icing- related incidents [e.g., 16, 17].

Aerodynamically critical parts that are prone to icing can be equipped with anti- and de-icing technology such as those using warm bleed air from engines, pneumatic boots or forcing freezing point depressant fluid out of porous panels [18]. Although such measures can reduce the ice formation or melt accreted ice, there is the potential risk of runback ice forming further downstream on unprotected areas. Heating and pneumatic systems often require complex configuration, adding weight and consuming power while de-icing fluids are expensive and the right type is not always available with the decision-making process strongly dependent on accurate icing hazard forecasts [19, 14, 20]. Currently, flight safety and costefficiency are addressed via development of better forecasting tools, remote sensing instruments, and protection measures. While forecasting tools and remote-sensing can facilitate hazard avoidance, protection measures have a direct impact on flight safety when avoidance is not possible.

With a drive towards more efficient and more electric aircraft systems, the energy budget available for the operation of traditional ice protection systems, e.g., heated leading edges, is reducing, consequentially, leading to an increasing need in alternative approaches for icing threat mitigation. Such prospective protection measures, currently being developed around the world, include icephobic coatings and ice accretion sensors. While the disruptive technology of icephobic coatings could offer a significant weight and power saving, the in-flight icing behavior is still far from being fully understood and needs to be thoroughly assessed using ground test facilities, modeling and in natural icing environment, when possible, before they can be considered a viable ice protection solution by aircraft manufacturers and regulatory authorities.

Icephobic coatings are meant to prevent ice accretion by reduction of ice adhesion to the substrate or suppression of ice formation altogether and can be applied and used as is (i.e., passive) or in tandem with heating applied to the surface (i.e., semi-passive), depending on several factors, such as: geometry of the surface, ambient temperature, wind speed and

direction, hydrometeor size and shape and other factors. In some cases, aerosol (small particulates suspended in the air) in high concentration interacting with the surface can also play a role, affecting the functionality, and therefore the efficiency, of icephobic surfaces.

NRC's Aerospace Research Center (ARC) specializes in icing studies. ARC's current projects include flights and collection of data in real icing environments, wind tunnel icing simulations, icing sensor development, modeling, and development of icephobic materials [e.g., <u>21-27</u>]. The In-Cloud Icing and Large-Drop Experiment (ICICLE) is one example of icing studies led by US Federal Aviation Administration (FAA) and conducted onboard NRC's Convair-580 aircraft [<u>28</u>], an airborne laboratory for atmospheric research, incorporating more than 40 probes and sensors for aircraft and atmospheric state, in-situ cloud (single-particle), cloud bulk properties, aerosol measurements and remote sensing [<u>21-24</u>, <u>29</u>].

While the study of icing conditions and ice accretion on different surfaces are ongoing in wind tunnels of different agencies around the world, such simulations are limited by the capabilities of the wind tunnels, which cannot represent the full complexity and range of the atmospheric particulates and dynamic mixing states. In addition, icing conditions covered by new regulations, e.g., SLD and ice crystals are difficult to recreate in current icing wind tunnel facilities and questions remain about the validity of the simulated environment compared to that experienced in flight [30]. Alternatively, models are often used to complement wind tunnel experiments; however, these are limited by computer power and the accuracy of parameterizations derived from historical measurements.

The aforementioned limitations can be addressed through the use of airborne platforms such as the NRC's Convair-580 that utilizes a high number and redundancy of probes and sensors. This aircraft offers multiple measurements during flight through natural icing conditions and provides data for comparison and validation of observations made using ground-based facilities and simulations.

Moreover, the limited testing options for unmanned aerial vehicles (UAV) in icing conditions [e.g., 31] may benefit from data collected with a large aircraft in severe icing, outside of the current flight envelope of UAVs. In this paper, we present new competencies of in-flight ice accretion analysis and protection through integration of in-house expertise in icing, sensing and materials. These new competencies will help to advance studies of aircraft icing and accelerate development of icing protection technologies in the coming years. In the following sections, we describe the characteristics and commissioning of a new airborne testing Platform for Ice-accretion and Coatings Tests with Ultrasonic Readings (PICTUR). A drawing of the PICTUR testing platform is shown in Figure 1.

Methods

For the design and flight tests of the PICTUR, we combined a unique overlap of airborne icing measurements expertise [e.g., 21, 22], in-house developed icephobic coatings [32, 26],

FIGURE 1 Left: Design drawing of PMS canister mounted PICTUR with two test articles; Right: Internal test article design, red custom-made heater with a temperature sensor in the middle.



and in-house developed icing sensors [33, 25], as well as modeling of ice accretion [34, 35]. In this section, we present the technical specifications of the new platform, and some relevant CFD simulations to evaluate its performance before commissioning. Next, we briefly describe the first set of coatings that were tested in icing flights. Finally, we describe the NRC Convair-580 research aircraft and provide a brief description of the flight conditions. In regard to aircraft data, we present only atmospheric, aircraft state, and cloud parameters, which are relevant for ice accretion analyses. These complementary aircraft data help to quantify the severity of icing, and to evaluate the performance of preventive measures, i.e., icephobic coatings.

PICTUR Specifications

The new PMS-canister mounted platform was designed with 2 symmetric Interchangeable test articles, in Port and Starboard locations relative to probe's longitudinal axis (Figure 2). The mountings of PICTUR were designed to allow for flexibility in test article geometries and structural materials. Normally, the geometry and composition of an airfoil would affect the airfield vectors, flow of particles towards the surface, and the accretion of ice. The current design can accommodate tests of separate surface geometries and materials of airfoils on each mounting. In particular, these engineering properties would have a critical role in comparisons of coated and uncoated reference areas. The current orientation of the PICTUR test articles was set by the spatial

FIGURE 2 An image of PICTUR integrated on the NRC Convair-580 aircraft, underwing Starboard Outer Lower (SOL) position.



constraints and the proximity to the carrying pylon and neighboring probes.

The test articles, currently aluminum cylinders, have forward facing surfaces coated with 4 coating samples with uncoated reference areas. Each coating is a rectangular of approximately 2" spanwise and 3" in circumference, curved around the forward-facing half of the cylinder (2.5" in diameter). The less aerodynamic design of the cylindrical test articles was chosen to maximize surface for ice accretion in flight and because its surface flow distribution, including Mach and Reynolds Number effects, are well understood [e.g., 36]. To observe the coatings, we included visual real-time inspection of the surface with two high-definition heated video cameras (1080p), which are mounted in the head of the probe facing aft, one for each test article.

The coated cylindrical test articles are equipped with internal heaters, which allow control of the surface temperature in flight, effectively from the ambient temperature up to 30 °C. The temperature control feature was added to allow for quick ice removal in between test periods in flight and to allow implementation of temperature stepping in the case of heat-assisted, semi-passive, icephobic protection coatings tests.

Another internally mounted component is an Ultrasonic Ice Accretion Sensor (UIAS) developed by the NRC. The sensor can detect surface ice in a non-intrusive manner [25]. It incorporates an array of detectors along each of the test articles, under coated and clear-aluminum reference areas. An algorithm is then applied to derive the detection of accretion, and preliminary quantification. In this study, data were acquired from PICTUR at a 1 Hz rate to facilitate synchronization with the complementary instruments onboard the aircraft. Table 1 provides a summary of all the characteristics of the PICTUR. The next section describes CFD simulations and analysis to evaluate performance.

CFD Simulations

Computational Fluid Dynamics (CFD) simulations of airflow and particle flow were used as a guidance in the development of an aerodynamic design of the canister mounted probe; evaluation of heat distribution on the cylindrical test articles;

TABLE 1 A Summary of PICTUR features.

Feature	Details	
Geometry of test articles	Currently cylinders, 2.5" diameter	
Orientation of test articles	Currently at 45 degrees	
Composition of test articles	Currently Aluminum (6061)	
Modularity	Test articles are self-contained and can have different designs	
Coatings	Currently 4 different icephobic coatings	
Surface measurements	UIAS for accretion detection, temperature	
Visual inspection and recording	Two 1080p HD cameras, 60 fps	
Complementary measurements when installed on NRC's Convair-580 aircraft	Core instruments that provide the atmospheric and aircraft state contextual information	

and assessment of the extent of ice accretion, comparing model with real data.

In-flight ice accretion is a complex phenomenon and challenging to simulate. The modelling, usually, involves 5 steps [37]. Once we established a computational model, we simulated changes in the angle of attack, wind speed, and hydrometeor size. The simulations also incorporated the heat-assisted operation mode to evaluate the extent of ice accretion in such settings.

In all CFD simulations, the probe was analyzed in isolation. For the aerodynamic design, the CFD software Cobalt, from Cobalt Solutions, LLC, was used while a combination of Ansys CFX and Ansys FENSAP-ICE were used for the heat distribution and ice accretion simulations. The same CFD model of the probe was analyzed in both the aerodynamic design and icing simulations.

Coatings

The test articles here were coated in preassigned locations, above UIAS detectors (Figure 3). The icephobic coatings applied to the test cylinders were formulated and tested by NRC. These are 2-component polyether urethane coatings that have superior erosion resistance against high-speed ice particles and rain droplets, as well as high surface hydrophobicity. Static water contact angles of the coatings are about 110°. For the coating applications, the aluminum surface was first treated using AkzoNobel's Metaflex SP 1050 pre-treatment, followed by application of a thin layer (ca. 20-25 microns) of non-chromate epoxy-based Aerodur HS 2118 CF primer. The NRC coatings were then spray-applied on top of the primer to provide a clear coat of about 100 µm in thickness. In this paper, we focus on the capabilities and preliminary observations obtained using the PICTUR platform without dwelling on the detailed analyses of chemistry, coating procedures, results intercomparison, and heat impact.

FIGURE 3 An example of a coated test article (Port side), which had 2 coating types.



Ultrasound Ice Accretion Sensor (UIAS)

The NRC has developed a non-intrusive, low-power, lightweight sensor that can be placed on the surface opposite to where the ice accretion is suspected of occurring (Figure 4). This technology uses ultrasound waves to detect accretion and is known as NRC Ultrasound Ice Accretion Sensors (UIAS) [25, 33]. The detection signal from these sensors changes in the presence of water or ice and has shown to be effective when some or all of the surface above the sensor gets covered. This technology was successfully demonstrated in a full scale ALF502R-5 aircraft engine, tested in altitude ice crystal icing (ICI) conditions led by NASA and the Ice Crystal Consortium (ICC) [25, 38-40]. As a follow-up to that test, a new generation of ultrasound ice accretion sensors were developed with improved functionality including the ability to detect accretion locally at the sensor but also in a larger area between sensors. This allowed a large area to be monitored for accretion with only a few sensors. This capability was proven in a vane segment test conducted at the NRC ICI test rig [33].

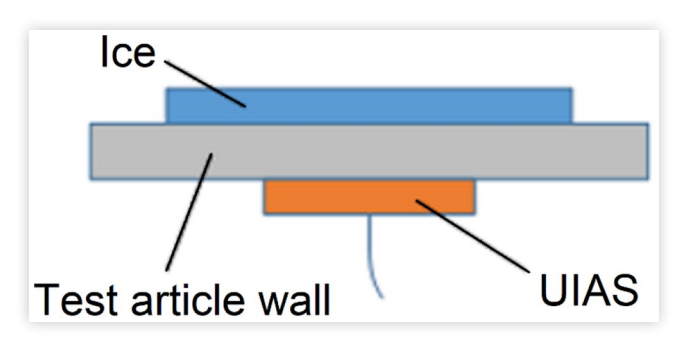
Some of this original work showed the UIAS was very sensitive to ice crystal icing, similar to the type of accretion seen with aircraft icing. It was therefore desirable to further examine and develop the UIAS capabilities in an aircraft-icing environment of supercooled water droplets. A series of UIAS sensors were installed on PICTUR to characterize ice accretion.

NRC Research Aircraft

The PICTUR was installed on NRC's Convair-580 aircraft. This is a twin-engine pressurized turbo-prop aircraft that has been extensively modified for research. A typical flight lasts 3 to 5 hours with maximal altitude of ~24,000 ft. This aircraft has been frequently used in icing research [e.g., 21, 41, 28, 29]. In addition to data collected with PICTUR, we employed aircraft sensors as complementary sources of information to target a variety of icing conditions (i.e., freezing drizzle, freezing rain, ice, and mixed-phase clouds).

The aircraft was instrumented with state-of-the-art in-situ and remote sensing instruments for cloud microphysical-properties measurements as well as aircraft state and atmospheric state parameters (Figure 5). Bulk water content

FIGURE 4 Schematic of ultrasound ice accretion sensors (UIAS) installed for ice accretion detection inside the test articles.



AIRBORNE PLATFORM FOR ICE-ACCRETION AND COATINGS TESTS WITH ULTRASONIC READINGS (PICTUR)

FIGURE 5 Picture of the NRC Convair-580 aircraft with some of the complementary instruments seen underwings.



was measured in tandem with single particle images and size distributions, ranging from small cloud droplets to large precipitation hydrometeors. For this work, cloud particle size distributions were collected from several single-particle commercial probes: Fast Cloud Droplet Probe (FCDP, 2-50 μm, SPEC Inc.); two-dimensional stereo probe (2DS, 10-1200 um, SPEC Inc.); High Volume Precipitation Spectrometer version 3 (HVPS3, 150-19200 µm, SPEC Inc.). In addition, Cloud Particle Imager (CPI, 10-2000 µm, SPEC Inc.) collected high resolution (~2 μm) grayscale imagery of small cloud and drizzle drops, ice crystals and portions of large drops and ice aggregates (see Appendix). Aerosol and water vapor data were collected as well. The full list of instruments that collected data during the flights is presented in Table A1 in the Appendix. More information about the aircraft and the equipment typically installed for flight campaigns can be found in published literature [e.g., 29, 23, 42, 43, 44].

Flights

Data have been collected during the FAA led winter flight campaign, January to February 2022, in the Northeast US. Those flights, primarily, targeted freezing rain (FZRA) and freezing drizzle (FZDZ) conditions, with a secondary emphasis on small drop icing conditions, to demonstrate and evaluate a new terminal area icing diagnostic and forecast tool. Typically, aircraft speed during data collection was between 80 to 100 m s⁻¹. The sampling strategy included leveled flights at different altitudes as well as missed approaches within the terminal areas. Next, we present some preliminary results from a number of flights.

Results

Freezing rain Glaze-ice accretion and runback over the test article were simulated using heat and mass transfer equations (FENSAP Ice, ANSYS Inc.). <u>Figure 6a</u> depicts simulation results for extreme glaze icing (20 min of accretion) and <u>Figure 6b</u> depicts a cross section at the mid-span of the test article.

In-flight, severe icing conditions were encountered. Figure 7 shows one of the test articles in clear-air and below it, the same test article in another flight, after few minutes of exposure to severe icing conditions as predicted in the simulations.

FIGURE 6 (a) Icing accretion (20 min @-10 °C, 100 m/s flow, MVD 1000 μ m, LWC 1 g m-³) and (b) Icing accretion on the cylinder at a cross section of the cylinder mid-span.

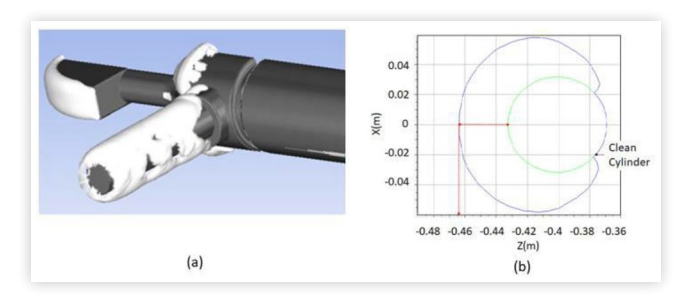
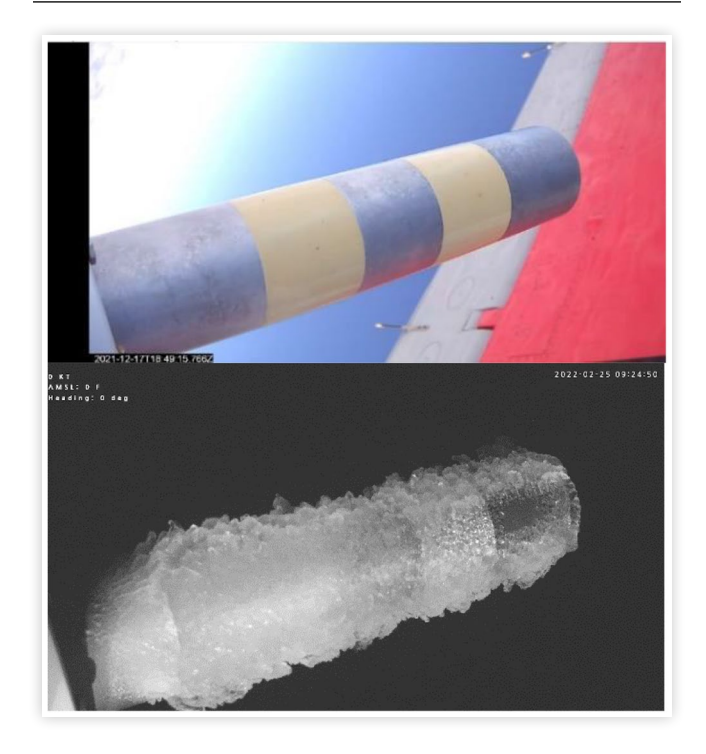


FIGURE 7 An example of icing encountered in flight. Top: Port test article in clear-air. Bottom: Port test article in another flight after several minutes in supercooled water drops (MVD $1000 \mu m$, LWC $0.9 g m^{-3}$).



A response of the UIAS signal to icing on the uncoated part of the test article, together with hydrometeor size distribution, is shown in Figure 8. In this example, the aircraft penetrated the cloud i.e. elevated liquid water content (LWC), around 20:36 when we start to observe temporal correlation between high concentration of supercooled small droplets and drizzle, mostly below 500 μm in diameter, which are causing the detected accretion. The signal remains constant while ice remains on the surface, without further accretion. Although results are preliminary, they provide confidence in UIAS ability to detect early supercooled water droplet accretion. Further work will be carried out to analyze the UIAS data over a range of ice accretion conditions and correlate them with measurements of the icing environment.

Another example of complementary indicators of icing periods in flight, derived from the Collins Rosemount Icing

FIGURE 8 Supercooled water drops accretion and detection example. Top panel: hydrometeor size distribution derived from CDP probe. Bottom panel: the resultant UIAS detection of ice accretion on both test articles (Port and Starboard) overlaid with LWC measured by Nevzorov and ICD sensors (see <u>Table A1</u> for details). The strongest spike in LWC leads to the sustained ice accretion detection by the UIAS.

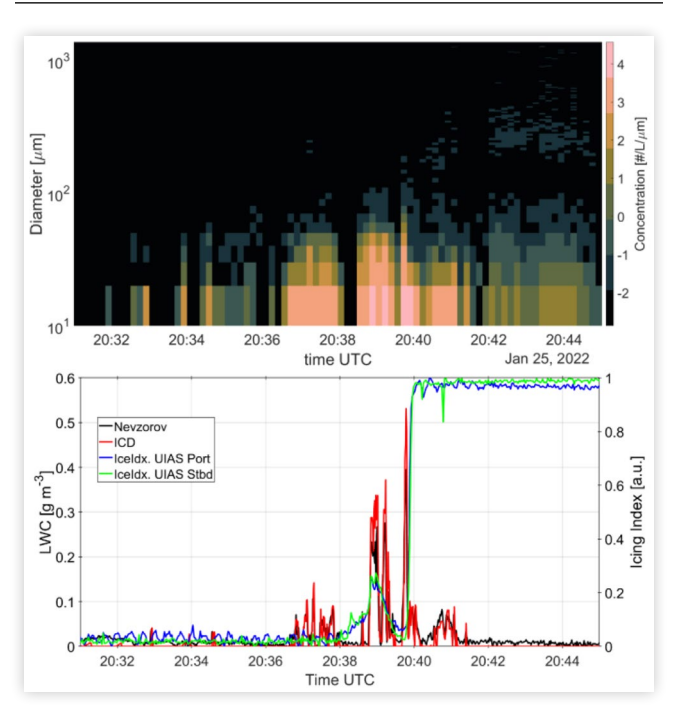
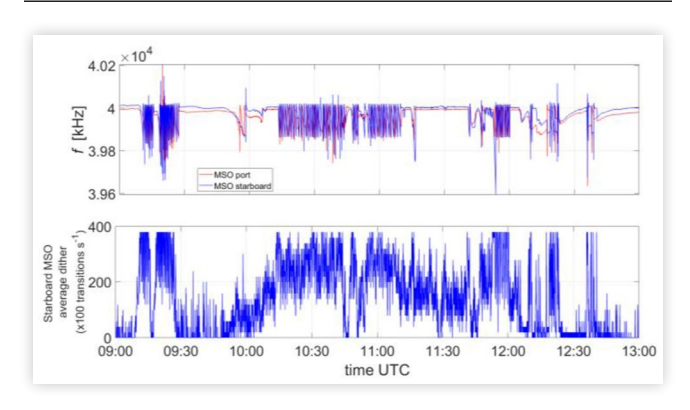


FIGURE 9 An example of icing conditions periods detected in one of the flights. Top panel: frequency shifts of 2 Collins Rosemount Icing Detectors. Bottom panel: Icing transitions observed using Collins' new dither algorithm.



Detectors onboard the NRC Convair-580 aircraft, shown in Figure 9. Examples of signals are shown from two icing detectors installed in port and starboard locations on the aircraft. The upper panel shows the raw frequency fluctuations, reflecting the ice accretion and shedding cycles with good correlation between the two detectors. The bottom panel uses an experimental dither algorithm from one of the detectors. The averaged dither parameter counts the average number of frequency changes per second and can also provide information about the non-freezing supercooled water portion [45].

In high intensity icing events there is a rough correlation between ice accretion rate, oscillator frequency and dither, restricted by the upper limit of ice shedding cycle frequency. In this example (<u>Figure 9</u>), there is a gradual increase in the intensity of ice accretion from 9:45 to 10:30 AM.

In <u>Figure 10</u>, we show an effective temperature control of a semi-assisted protection heat-stepping applied during one of the many icing flights (black) and the corresponding feedback readings of the test article surface temperature from both test articles in flight. Set temperature is reached at the center of the test section on the test article and it is significantly lower in the canister attachment joints (blue).

An example of other typical complementary information of the atmospheric environment and aircraft state is shown in <u>Figure 11</u>. These include: true air speed, static air temperature, static air pressure, and water vapor concentration.

Next, we show a composite size-distribution time series for the same flight (<u>Figure 12</u>). The uncertainties of diameter derivation from imaged projections, corrections of interarrival time, sample area definition, area ratio correction that were applied are described in detail in [46].

In Figure 13, we show the distribution of median volume diameters (MVD) relative to the maximum observed diameter (D_{max}) throughout the same flight as shown in Figure 12. Time series of one of the flight segments, dominated by SLD conditions, is shown in the lower panel of Figure 13. Drop diameters reach well above 1 mm and sometimes above 1 cm at the static temperature of -5 °C.

FIGURE 10 An example of time series of two test articles surface temperatures, color-coded (top and bottom panels, Port and Starboard locations respectively). Black line: Set temperature for each of the test articles. Test article temperature middle-location (red line) and temperature reading location near-canister (blue line).

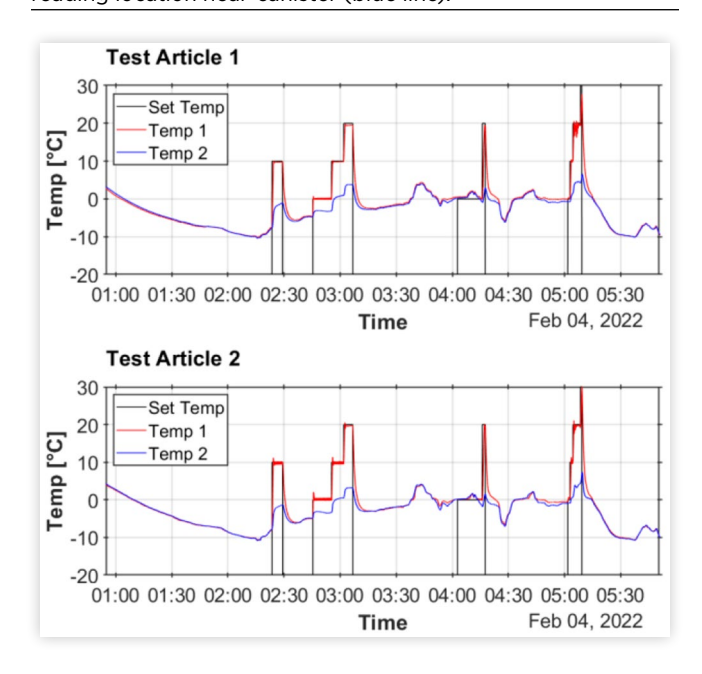


FIGURE 11 An example of selected atmospheric and aircraft state information collected in one of the icing flights. Top left: aircraft true air speed, Top right: Static air temperature, Bottom left: Static air pressure, Bottom right: Water vapor concentration.

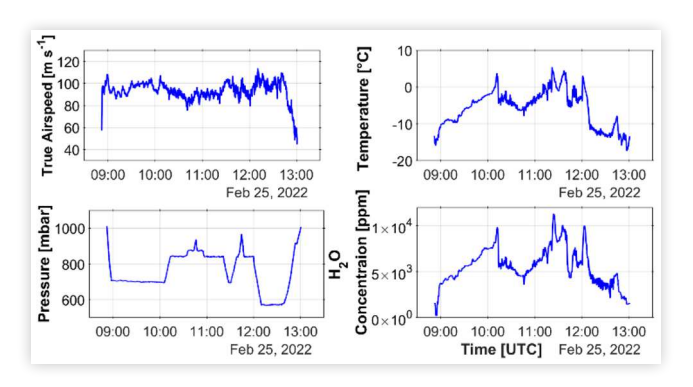
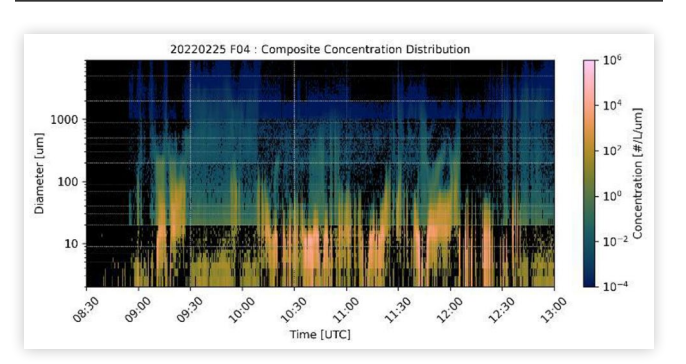


FIGURE 12 An example of composite size distribution of hydrometeors combined from scattering and optical array probes detected concentration. Single particle images of FZRA conditions are presented in the appendix.

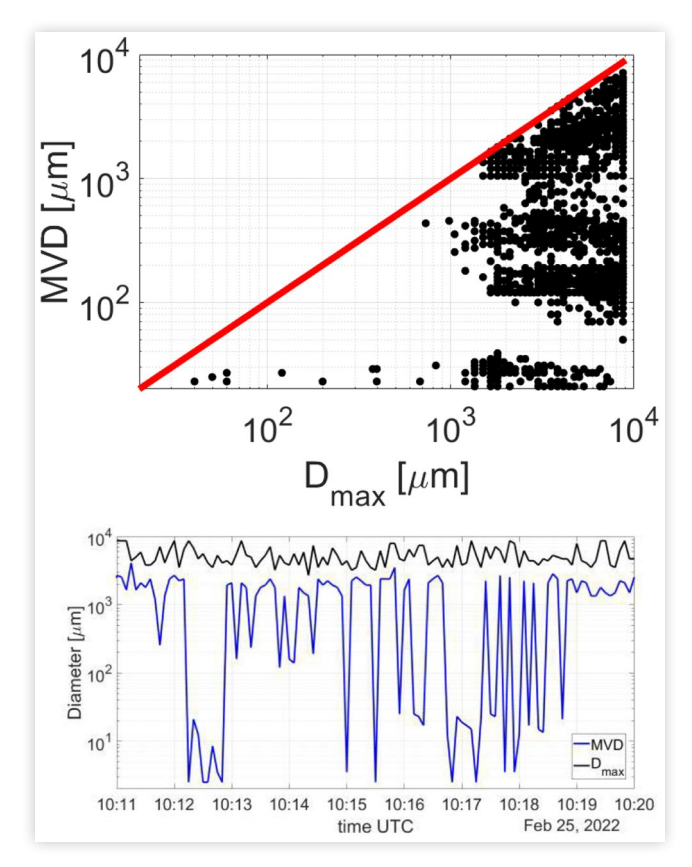


Discussion and Summary

In this paper, we have presented a novel airborne platform for aircraft icing studies and ice protection solutions tests in natural atmospheric icing environments. We have demonstrated the operation of the platform in a variety of icing conditions encountered in targeted FAA-led flights. The platform provides both visual observations and surface icing detection. The controllable temperature stepping makes it possible to assess energy efficiency of semi-passive coating systems. The modular insert design allows easy geometry shifts in the future as well as surface modifications to evaluate different icephobic coatings on various prototypes of airfoil structures. Last but not least, PICTUR coupled with comprehensive environmental data collected from probes, installed on NRC's Convair-580 aircraft, enable effective correlation of atmospheric conditions to the icing and ice protection properties of surfaces under evaluation, as demonstrated in this paper.

Here, we showed some preliminary exemplary results of ice accretion visual observations caused by supercooled water drops and an example of ice accretion detection with the UIAS. Overall, good correlation of ice accretion initiation was observed between Collins Rosemount Icing Detector readings

FIGURE 13 MVD and D_{max} observed during the flight in Figure 12. Top panel: MVD vs. D_{max} for the whole flight, red line indicates 1:1 ratio. Bottom panel: time series of a flight segment with predominantly FZRA/SLD (>1 mm) conditions.



and UIAS readings. The occurrences of unique icing conditions are supported by single particle imagery and temperature data (Figures 11, A1). Figure 12 shows the concentration size distribution of hydrometeors throughout one of the icing flights. The liquid water content measured by the Nevzorov, often used in wind tunnel tests, has known limitations due to its collection efficiency in Appendix O icing conditions [47]. Figure 13 demonstrates the importance of the complementary measurements from the optical array probes which can be used for derivation of the true LWC over the full-size spectrum (2 μm – 2 cm), in particular in FZRA icing.

In these preliminary results, we noticed that in FZRA events some of the tested coatings play an important role in reduction of ice accretion on the leading edge, although the size of the rain drops and their velocity vector, perpendicular to flight propagation, may cause drop deformation and vary the splashing and liquid runback on the coatings, therefore changing protection efficiency in different aircraft types [e.g., 48, 49]. These results of coatings protection efficiency analysis will be reported in the following months.

The high cost, risk, and complexity of flying in unique and inimitable atmospheric icing conditions, often inhibit studies of this nature, which are, nonetheless, essential to understand in-flight icing in real, convoluted, dynamic environments and to test prospective icing protection solution candidates. The unique datasets collected will help to advance knowledge in ice protection, validate and fine-tune existing

icing simulation algorithms, and accelerate development of innovative icephobic surfaces and icing sensors. Moreover, this study and its follow-ups will strive to identify materials and further develop detection technologies also applicable to wind turbines, power lines, bridges and other infrastructure.

Lastly, aerosol is rarely, if at all, taken into account in wind tunnel icing studies and simulations however, it may have a significant role in real flight environment (e.g., salt particulates that suppress the freezing point of water or hydrophobic black carbon and ash flakes, or oily organic aerosol). For example, during missed approaches or takeoffs, periods of increased vulnerability, the surface aerosol concentration in the air can get quite high, especially during cold winter heating seasons. These nanoparticles have the ability to alter ice adhesion efficiency on protective surfaces. In the next steps, aerosol data collected in these flights will be crosschecked with other datasets to assess its impact on icing, in particular in cases of low altitude FZRA precipitation.

References

- Yamazaki, M., Jemcov, A., and Sakaue, H., "A Review on the Current Status of Icing Physics and Mitigation in Aviation," *Aerospace* 8 (2021): 188, doi: https://doi.org/10.3390/aerospace8070188.
- 2. Federal Aviation Administration, "Appendix C to Part 25. U.S. Code of Federal Regulations, Title 14, Chapter I, Subchapter C, Part 25, Appendix C," 2021, https://www.govinfo.gov/app/details/CFR-2021-title14-vol1/CFR-2021-title14-vol1-part25-appC.
- National Transportation Safety Board, "In-Flight Icing Encounter and Loss of Control Simmons Airlines, d. b. a. American Eagle Flight 4184 Avions de Transport Regional (ATR) Model 72-212, N401AM, Roselawn, Indiana," NTSB/ AAR-96/01, 1994.
- Miller, D., Ratvasky, T., Bernstein, B., McDonough, F. et al., "NASA/FAA/NCAR Supercooled Large Droplet Icing Flight Research: Summary of Winter 96-97 Flight Operations," in Proceeding AIAA 36th Aerospace and Science Meeting and Exhibit, Reno, NV, AIAA 1998-0577, 1997.
- 5. Curry, J.A., Hobbs, P.V., King, M.D., Randall, D.A. et al., "FIRE Arctic Clouds Experiment," *Bulletin of the American Meteorological Society* 81 (2000): 5-29.
- Cober, S.G., Isaac, G.A., and Strapp, J.W., "Characterisation of Aircraft Icing Environments that Include Supercooled Large Drops," *Journal of Applied Meteorology* 40 (1984-2002).
- Isaac, G.A., Cober, S.G., Strapp, J.W., Korolev, A.V. et al., "Recent Canadian Research on Aircraft In-flight Icing," Canadian Aeronautics and Space Journal 47, no. 3 (2001).
- Isaac, G.A., Cober, S.G., Strapp, J.W., Hudak, D. et al., "Preliminary Results from the Alliance Icing Research Study (AIRS)," in *Proceeding AIAA 39th Aerospace and Science Meeting and Exhibit*, Reno, NV, AIAA 2001-0393, 2001.
- 9. Federal Aviation Administration, "Airplane and Engine Certification Requirements in Supercooled Large Drop, Mixed Phase and Ice Crystal Icing Conditions; Final Rule. 14

- CFR Parts 25 and 33. Federal Register, vol. 79, no. 213, 34, 2014
- Federal Aviation Administration, "Appendix O to Part 25 -Supercooled Large Drop Icing Conditions. U.S. Code of Federal Regulations, Title 14, Chapter I, Subchapter C, Part 25, Appendix O," 2021, https://www.govinfo.gov/app/details/CFR-2021-title14-vol1-part25-appO.
- Mazzawy, R. and Strapp, J., "Appendix D An Interim Icing Envelope," SAE Technical Paper <u>2007-01-3311</u>, 2007, doi:https://doi.org/10.4271/2007-01-3311.
- 12. Federal Aviation Administration, "Appendix D to Part 33 Mixed Phase and Ice Crystal Icing Envelope (Deep Convective Clouds). U.S. Code of Federal Regulations, Title 14, Chapter I, Subchapter C, Part 33, Appendix D," 2021, https://www.govinfo.gov/app/details/CFR-2021-title14-vol1/CFR-2021-title14-vol1-part33-appD.
- 13. European Aviation Safety Agency, "Certification Specifications and Acceptable Means of Compliance for Large Aeroplanes, Appendix P, Admt 18," 2016.
- Transportation Safety Board of Canada (TSB), "Air Transportation Safety Issue Investigation Report A15H0001," released November 7, 2019.
- 15. Petty, K.R. and Floyd, C.D.J.: "A Statistical Review of Aviation Airframe Icing Accidents in the U.S," in 11th Conference on Aviation, Range, and Aerospace, Aviation Accident and Incident Reviews, October 3-7, 2004.
- NTSB (National Transportation Safety Board) US, "Office of Aviation Safety," Meteorology Factual Report, WPR19FA154, Washington, DC, January 19, 2021.
- ROSAVIATSIA (Federal Air Transport Agency of Russian Federation), "Accident Report 1892/03. For Aircraft A321 -27IN VQ-BGU of Siberia Airlines, 24-12-2021." (in Russian), accessed April 4, 2022, https://aviaforum.ams3.cdn.digitaloceanspaces.com/data/attachment-files/2022/01/1659736 c08e2316ec004d1cf7ab9afa500f4e2c. pdf
- Federal Aviation Administration, "Advisory Circular 91-74B Pilot Guide: Fight in Icing Conditions," 2015.
- 19. European Aviation Safety Agency (EASA) RMT.0572, "Use of Comparative Analysis When Showing Compliance with SLD Icing Specifications," Notice of Proposed Amendment, June 2015.
- Elliott, J.W. and Smith, F.T., "Ice Formation on a Smooth or Rough Cold Surface Due to the Impact of a Supercooled Water Droplet," *Journal of Engineering Mathematics*, 2015, doi:10.1007/s10665-015-9784-z.
- Williams, E.R., Donovan, M.F., Smalley, D.J., Kurdzo, J.M. et al., "The 2017 Buffalo Area Icing and Radar Study (BAIRS II)," Project Report ATC-447, May 2020.
- Strapp, J., Schwarzenboeck, A., Bedka, K., Bond, T. et al., "Comparisons of Cloud In Situ Microphysical Properties of Deep Convective Clouds to Appendix D/P Using Data from the High-Altitude Ice Crystals-High Ice Water Content and High Ice Water Content-RADAR I Flight Campaigns," SAE Int. J. Aerosp. 14, no. 2 (2021): 127-159, doi: https://doi. org/10.4271/01-14-02-0007.
- 23. Wolde, M., Nguyen, C., Korolev, A., and Bastian, M., "Characterization of the Pilot X-Band Radar Responses to the HIWC Environment during the Cayenne HAIC-HIWC

- 2015 Campaign," In in 8th AIAA Atmospheric and Space Environments Conference, Washington, DC, June 13-17, 2016, doi:10.2514/6.2016-4201.
- 24. Nguyen, C.M., Wolde, M., and Korolev, A., "Determination of Ice Water Content (IWC) in Tropical Convective Clouds from X-Band Dual-Polarization Airborne Radar," *Atmos. Meas. Tech.* 12 (2019): 5897-5911, doi:https://doi.org/10.5194/amt-12-5897-2019.
- Fuleki, D., Zhigang, S., Wu, J., and Miller, G., "Development of a Non-Intrusive Ultrasound Ice Accretion Sensor to Detect and Quantify Ice Accretion Severity," in 9th AIAA Atmospheric and Space Environments Conference, 2017, https://doi.org/10.2514/6.2017-4247.
- Song, N. and Benmeddour, A., "Durable Icephobic Coatings for Aerospace Applications," LTR-AMTC-2019-0071, NRC, 2019.
- Orchard, D., Clark, C., and Oleskiw, M., "Development of a Supercooled Large Droplet Environment within the NRC Altitude Icing Wind Tunnel," SAE Technical Paper <u>2015-01-2092</u>, 2015, doi:https://doi.org/10.4271/2015-01-2092.
- 28. Bernstein, B., DiVito, S., Riley, J.T., Landolt, S. et al., "The In-Cloud Icing and Large-Drop Experiment Science and Operations Plans," [DOT/FAA/TC-21/29], Atlantic City International Airport, NJ: Federal Aviation Administration, 2021, https://doi.org/10.21949/1524472.
- 29. Nguyen, C.M., Wolde, M., Battaglia, A., Nichman, L. et al., "Coincident in situ and Triple-Frequency Radar Airborne Observations in the Arctic," *Atmos. Meas. Tech.* 15 (2022): 775-795, doi:https://doi.org/10.5194/amt-15-775-2022.
- 30. Orchard, D., Szilder, K., and Davison, C., "Design of an Icing Wind Tunnel Contraction for Supercooled Large Drop Conditions," AIAA 2018-3185, Atlanta, Georgia, 2018.
- 31. Siddique, M., Han, N., and Hu, H., "Development of an Experimental Unmanned-Aerial System (UAS) to Study the Effects of Adverse Weathers on its Flight Performance," AIAA 2022-1646, AIAA SCITECH 2022 Forum, January 2022.
- Benmeddour, A. and Song, N., "Durable Icephobic Coatings for Shipborne UAVs," Technical Report LTR-AL-2021-0015, National Research Council Canada, 2021.
- Fuleki, D., Sun, Z., Wu, J., Lothrop, A. et al., "Implementation of a Non-Intrusive Ultrasound Ice Accretion Sensor to an ALF502R-5 Vane Segment Ice Crystal Component Test," Atmospheric and Space Environments. American Institute of Aeronautics and Astronautics, 2022, https://doi.org/10.2514/6.2022-3697.
- 34. Szilder, K. and Lozowski, E.P., "Three-Dimensional Numerical Simulation of Ice Accretion using a Discrete Morphogenetic Approach," in in 9th AIAA Atmospheric and Space Environments Conference, Denver, Colorado, USA, June 5-9, 2017, doi:10.2514/6.2017-3418
- Szilder, K. and Lozowski, E.P., "Novel Two-Dimensional Modelling Approach for Aircraft Icing," AIAA Journal of Aircraft 41, no. 4 (2004).
- 36. Koss, H.H., Gjelstrup, H., and Georgakis, C.T., "Experimental Study of Ice Accretion on Circular Cylinders at Moderate Low Temperatures," *Journal of Wind Engineering and Industrial Aerodynamics* 104–106 (2012): 540-546, doi:https://doi.org/10.1016/j.jweia.2012.03.024.

- Caminade, F., Frazza, L., Onera-Rouzad, O., and Trontin, P.,
 "Definition of Numerical Capability Requirements for Liquid Icing Conditions," Deliverable D3.4, Ice Genesis, 2019
- 38. Goodwin, V.R. and Dischinger, D.G., "Turbofan Ice Crystal Rollback Investigation and Preparations Leading to Inaugural Ice Crystal Engine Test at NASA PSL-3 Test Facility," in 6th AIAA Atmospheric and Space Environments Conference, 2014, doi:10.2514/6.2014-2895
- Goodwin, R.V. and Fuleki, D., Engine Preparation and Instrumentation for the Second Ice Crystal Engine Test at NASA PSL-3 Test Facility (Washington DC: AIAA, 2016)
- 40. Flegel, A.B. and Oliver, M.J., "Preliminary Results from a Heavily Instrumented Engine Ice Crystal Icing Test in a Ground Based Altitude Test Facility," in 8th AIAA Atmospheric and Space Environments Conference, 2016, doi:10.2514/6.2016-3894
- 41. Huang, Y., Wu, W., McFarquhar, G.M., Wang, X. et al., "Microphysical Processes Producing High Ice Water Contents (HIWCs) in Tropical Convective Clouds during the HAIC-HIWC Field Campaign: Evaluation of Simulations Using Bulk Microphysical Schemes," *Atmos. Chem. Phys.* 21 (2021): 6919-6944, doi:https://doi.org/10.5194/acp-21-6919-2021.
- Baibakov, K., Wolde, M., Nguyen, C., Korolev, A. et al., "Performance of a Compact Elastic 355 nm Airborne Lidar in Tropical and Mid-Latitude Clouds," in Proceeding SPIE 10006, Lidar Technologies, Techniques, and Measurements for Atmospheric Remote Sensing XII, 100060C, October 24, 2016, https://doi.org/10.1117/12.2242112
- 43. Baibakov, K., LeBlanc, S., Ranjbar, K., O'Neill, N.T. et al., "Airborne and Ground-Based Measurements of Aerosol Optical Depth of Freshly Emitted Anthropogenic Plumes in the Athabasca Oil Sands Region," *Atmos. Chem. Phys.* 21 (2021): 10671-10687, doi:https://doi.org/10.5194/acp-21-10671-2021.
- 44. Nichman, L., Bliankinshtein, N., Wolde, M., Davison, C. et al., "Advanced Techniques for Airborne Measurements Tested Onboard NRC's Convair-580 Aircraft," in *International Conference on Clouds and Precipitation, ICCP 2021*, August 2-6, 2021, Pune, India, https://tinyurl.com/iccpconvair
- 45. Jackson, D.G., Anderson, K.J., and Heuer, W.D., "Liquid Water Detection Algorithm for the Magnetostrictive Ice Detector," SAE Technical Paper 2023-01-1430, 2023.
- 46. McFarquhar, G.M., Baumgardner, D., Bansemer, A., Abel, S.J. et al., "Processing of Ice Cloud in Situ Data Collected by Bulk Water, Scattering, and Imaging Probes: Fundamentals, Uncertainties, and Efforts toward Consistency," Meteorological Monographs 58 (2017): 11.1-11.33, doi:10.1175/AMSMONOGRAPHS-D-16-0007.1.
- Esposito, B., Orchard, D., Lucke, J., Nichman, L. et al., "Comparability of Hot-Wire Estimates of Liquid Water Content in SLD Conditions," SAE Technical Paper 2023-01-1423, 2023.
- 48. Burzynski, D., Roisman, I., and Bansmer, S., "On the Splashing of High-Speed Drops Impacting a Dry Surface," *Journal of Fluid Mechanics* 892 (2020): A2, doi:10.1017/jfm.2020.168.

49. Fortin, G., "Super-Hydrophobic Coatings as a Part of the Aircraft Ice Protection System," SAE Technical Paper 2017-01-2139, 2017, https://doi.org/10.4271/2017-01-2139.

Contact Information

Leonid.Nichman@nrc.ca

Acknowledgments

We thank the pilots (Anthony Brown, Bryan Carrothers, Reagh Sherwood), engineering, operation, and managerial staff from NRC FRL Instrumentation, in particular Ovenden Mark, Eric Roux, Steve Ingram, NRC Design and Fabrication Services Robert Macey, Airworthiness team. The project received funding from the following NRC programs: Ideation New Beginnings, Aerospace Futures Initiative (AFI), Aeronautical Product Development and Certification (APDC) program and leveraged shared resources from the FAA TAIWIN icing program and the National Science Foundation (NSF) Division of Atmospheric and Geospace Sciences grant no. 2113995. We also would like to thank Thomas Ratvasky (NASA) for letting us use the Cloud Particle Imager, and SPEC Inc. for the loan of the HVPS-3 probe.

Definitions/Abbreviations

2DS - 2D Stereo Probe

ARC - Aerospace Research Center, NRC

CFD - Computational Fluid Dynamics

CFR - Code of Federal Regulations

CPI - Cloud Particle Imager

CS - Certification Specifications

DAS - Data Acquisition System

EASA - European Union Aviation Safety Agency

FAA - US Federal Aviation Administration

FCDP - Fast Cloud Droplet Probe (SPEC Inc.)

FZDZ - Freezing Drizzle

FZRA - Freezing Rain

HIWC - High Ice Water Content

HVPS-3 - High Volume Precipitation Spectrometer version 3 (SPEC Inc.)

ICD - Icing Conditions Detector (SEA WCM-2000)

ICC - Ice Crystal Consortium

ICI - Ice Crystal Icing

ICICLE - In-Cloud Icing and Large-Drop Experiment (flight campaign)

LWC - Liquid Water Content

MVD - Median Volume Diameter

MSO - Magnetostrictive Oscillator

MVD - Median Volume Diameter

NAW - NRC Airborne W-band radar

NRC - National Research Council Canada

OAP - Optical Array Probe

PICTUR - Platform for Ice-accretion and Coatings Tests with Ultrasonic Readings

PIL - Port Inner Lower (location)

PMS - Particle Measuring Systems (company)

POU - Port Outer Upper (location)

PSP - Port Single Pylon (location)

RH - Relative Humidity

RID - Collins Goodrich/Rosemount Icing Detector

SIL - Starboard Inner Lower (location)

SLD - Supercooled Large Drops

SOL - Starboard Outer Lower (location)

SOU - Starboard Outer Upper (location)

SSP - Starboard Single Pylon (location)

STBD - Starboard (location)

SUW - Starboard Under Wing (location)

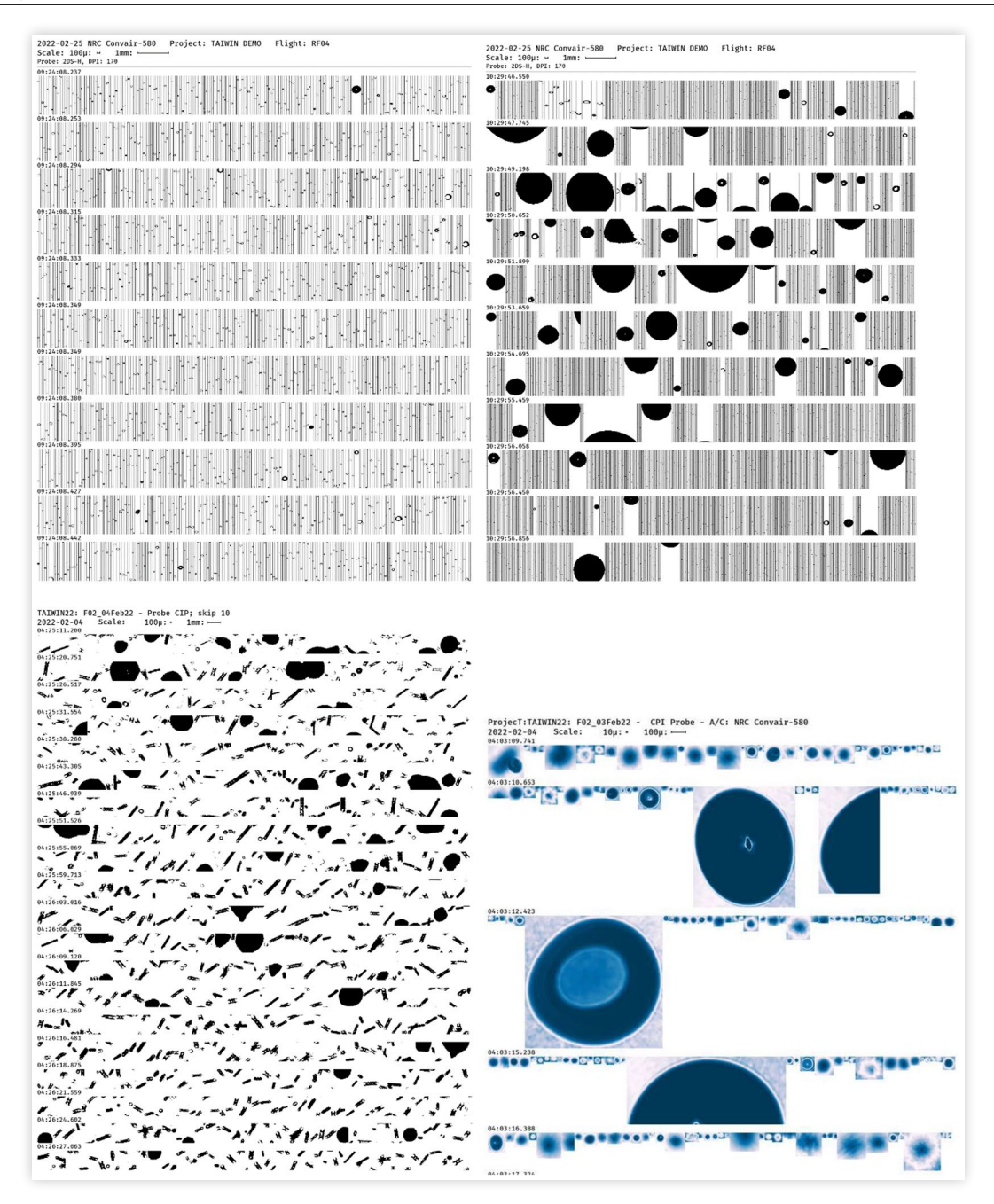
TWC - Total Water Content

UAV - Unmanned Aerial Vehicles

UIAS - Ultrasonic Ice Accretion Sensor

Appendix

FIGURE A1 Single particle images collected in sub-zero temperatures in flight (i.e., FZRA, FZDZ, ice). Images from CIP, CPI, 2DS (see <u>Table A1</u>).



Below, <u>Table A1</u> lists all the core instrumentation that was installed on the NRC Convair-580 aircraft during the flight tests and the complementary data available for evaluation of the flight environment.

TABLE A1 A list of relevant instruments operated on NRC Convair-580 aircraft in icing flights.

Probe/Sensor	Location	Description	Additional info
GPS	Fuselage	Aircraft state parameters	
PICTUR	SOL	Icing video and ultrasonic readings	
RMNT858	SOU	Winds, Pressure, Temperature	
LICOR 7000	Cabin inlet	Water Vapour, RH	
LICOR 840a	Cabin inlet	Water Vapour, RH	
Chilled mirror Hygrometer	Cabin Inlet	RH, Td	
RID	PSB	Icing	[1]
RID	SUW	Icing and accreted non-freezing phase	[1]
Nevzorov	STBD scalarboom	LWC, TWC	[2]
ICD	Fuselage starboard	TWC	[<u>3</u>]
FCDP	SIL	Droplets 2-50 μm	<u>[4]</u>
2DS	SIL	Imaging of Hydrometeors 10- 1200 µm	<u>[5]</u>
CIP-15	POU	Imaging of Hydrometeors 15- 960 µm	
HVPS-3	PIL	Imaging of Hydrometeors 150- 19200 µm	[6]
CPI v2.5	SSP	Imaging of hydrometeors 10- 2000, res 2.3 µm	[7]
Particle-I	PSP	Imaging of hydrometeors 10- 2000 µm	[8]
NAW	Fuselage	Remote sensing W-band radar	[<u>9</u>]
AECL lidar	Fuselage	Zenith 355 nm lidar	[10]

Appendix References

 Jackson, D.G., Anderson, K.J., and Heuer, W.D., "Liquid Water Detection Algorithm for the Magnetostrictive Ice Detector," SAE Technical Paper <u>2023-01-1430</u>, 2023.

- Korolev, A.V., Strapp, J.W., Isaac, G.A., and Nevzorov, A.N., "The Nevzorov Airborne Hot-Wire LWC-TWC Probe: Principle of Operation and Performance Characteristics," *J. Atmos. Oceanic Technol.* 15 (1998): 1495-1510, doi:10.1175/1520-0426(1998)015<1495:TNAHWL>2.0.CO;2.
- 3. Lilie, L.E., Bouley, D., Sivo, C.P., and Ratvasky, T.P., "Test Results for the SEA Ice Crystal Detector (ICD) under SLD Conditions at the NASA IRT," AIAA 2021-2654. AIAA AVIATION 2021 FORUM, August 2021.
- 4. Lawson, P., Gurganus, C., Woods, S., and Bruintjes, R., "Aircraft Observations of Cumulus Microphysics Ranging from the Tropics to Midlatitudes: IMPLICATIONS for a "New" Secondary Ice Process," *J. Atmos. Sci.* 174 (2017): 2899-2920, doi:10.1175/JAS-D-17-0033.
- Lawson, R.P., O'Connor, D., Zmarzly, P., Weaver, K. et al., "The 2D-S (Stereo) Probe: Design and Preliminary Tests of a New Airborne, High-Speed, High-Resolution Particle Imaging Probe," *J. Atmos. Oceanic Technol.* 23 (2006): 1462-1477, doi:10.1175/JTECH1927.1.
- 6. "SPEC HVPS V3 Technical Manual (Rev. 1.2)," 2013. Last accessed online June 17, 2022.
- Lawson, R.P., Baker, B.A., Schmitt, C.G., and Jensen, T.L., "An Overview of Microphysical Properties of Arctic Clouds Observed in May and July 1998 during FIRE ACE," *J. Geophys. Res.* 106 (2001): 14989-15014, doi:10.1029/2000JD900789.
- 8. Bachalo, W.D., Strapp, J.W., Biagio, E., Korolev, A. et al., "Performance of the Newly Developed High Speed Imaging (HSI) Probe for Measurements of Size and Concentration of Ice Crystals and Identification of Phase Composition of Clouds," in SAE 2015 Int. Conf. on Icing of Aircraft, Engines, and Structures (Prague, Czech Republic: SAE), 2015.
- 9. Wolde, M., Battaglia, A., Nguyen, C., Pazmany, A.L. et al., "Implementation of Polarization Diversity Pulse-Pair Technique Using Airborne W-Band Radar," *Atmos. Meas. Tech.* 12 (2019): 253-269, doi:https://doi.org/10.5194/amt-12-253-2019.
- Baibakov, K., Wolde, M., Nguyen, C., Korolev, A. et al., "Performance of a Compact Elastic 355 nm Airborne Lidar in Tropical and Mid-Latitude Clouds," in Proceeding SPIE 10006, Lidar Technologies, Techniques, and Measurements for Atmospheric Remote Sensing XII, 100060C, 2016, https://doi. org/10.1117/12.2242112

2023 SAE International; His Majesty the King in Right of Canada as represented by the National Research Council of Canada. This is the work of a government and is not subject to copyright protection. Foreign copyrights may apply. The government under which this work was written assumes no liability or responsibility for the contents of this work or the use of this work, nor is it endorsing any manufacturers, products, or services cited herein and any trade name that may appear in the work has been included only because it has been deemed essential to the contents of the work.